Ultrastrong extraordinary transmission and reflection in PT-symmetric periodic triangle optical waveguide networks

Xu-Bo Hu(胡旭波), Xian Zhang(张娴), Xiang-Bo Yang(杨湘波)

Citation: Chin. Phys. B. 35, 104205 (2026). DOI: 10.1088/1674-1056/ae5809 | CSTR: 32038.14.CPB.ae5809
http://cpb.iphy.ac.cn; http://iopscience.iop.org/cpb

What follows is a list of articles you may be interested in

Heterogeneous integration of silicon nitride photonics and CVD-grown WS_2 for second harmonic generation

Xuhang Jia(贾旭航), Bangren Xu(许邦仁), Jieyi Luo(罗劼舣), Ning Liu(刘宁), Yuhang Wang(王宇航), Biyuan Zheng(郑弼元), Wei Xu(徐威), Ken Liu(刘肯)
Chin. Phys. B. 34, 074205 (2025). DOI: 10.1088/1674-1056/adc7f7 | CSTR: 32038.14.CPB.adc7f7

Enhanced sensing of anharmonicities in a gain-based anti-PT symmetric system

Ya-Wei Zeng(曾亚伟), Tian-Le Yang(杨天乐), Qi-Yin Lin(林琪茵), Wan-Jun Su(苏万钧)
Chin. Phys. B. 33, 124201 (2024). DOI: 10.1088/1674-1056/ad8a4d

Controlling multiple optomechanically induced transparency in the distant cavity-optomechanical system

Rui-Jie Xiao(肖瑞杰), Gui-Xia Pan(潘桂侠), Xiao-Ming Xiu(修晓明)
Chin. Phys. B. 30, 034209 (2021). DOI: 10.1088/1674-1056/abc7a4

Extraordinary propagation characteristics of electromagnetic waves in one-dimensional anti-*PT*-symmetric ring optical waveguide network

Jie-Feng Xu(许杰锋), Xiang-Bo Yang(杨湘波), Hao-Han Chen(陈浩瀚), Zhan-Hong Lin(林展鸿)
Chin. Phys. B. 29, 064201 (2020). DOI: 10.1088/1674-1056/ab8371

Extraordinary transmission and reflection in *PT*-symmetric two-segment-connected triangular optical waveguide networks with perfect and broken integer waveguide length ratios

Jia-Ye Wu(吴嘉野), Xu-Hang Wu(吴栩航), Xiang-Bo Yang(杨湘波), Hai-Ying Li(李海盈)
Chin. Phys. B. 28, 104208 (2019). DOI: 10.1088/1674-1056/ab3f92

Ultrastrong extraordinary transmission and reflection in PT-symmetric periodic triangle optical waveguide networks

Xu-Bo Hu(胡旭波)[1,†], Xian Zhang(张娴)[2], and Xiang-Bo Yang(杨湘波)[2,‡]

[1] *College of Artificial Intelligence and Low-altitude Technology, South China Agricultural University, Guangzhou* 510642, *China*
[2] *Guangdong Provincial Key Laboratory of Nanophotonic Functional Materials and Devices, School of Information and Optoelectronic Science and Engineering, South China Normal University, Guangzhou* 510006, *China*

(Received 21 December 2025; revised manuscript received 24 February 2026; accepted manuscript online 27 March 2026)

We investigate the ultrastrong extraordinary transmission and reflection in the PT-symmetric periodic triangular optical waveguide network (PTSPTOWN). It is found that the extremum boundary points of photonic modes can be identified after reclassifying photonic modes. At the extremum boundary points of photonic modes, this network can generate ultrastrong extraordinary transmission and reflection, whose values can all arrive at the order of magnitude of 10^{11} and are six orders of magnitude larger than that produced by aperiodic networks. We introduce the effective refractive index to explain the mechanism of generating extraordinary optical characteristics and find that the total gain and loss effect of this network defined by the imaginary part of the effective refractive index is exactly corresponding to the ultrastrong extraordinary transmission and reflection, but there is no clear correspondence between the group index of this network defined by the real part of the effective refractive index and the ultrastrong extraordinary transmission and reflection. It may deepen people's knowledge on PT-symmetric periodic optical waveguide networks and may be useful for the designing of extremely narrow filters, optical switches, high-efficient photon storage, and other all-optical devices.

Keywords: optical waveguide network, PT-symmetric, optical materials, metamaterials

PACS: 42.25.Bs, 42.79.Gn, 11.30.Er

DOI: 10.1088/1674-1056/ae5809 **CSTR:** 32038.14.CPB.ae5809

1. Introduction

Parity-time-symmetric (PT-symmetric) optical systems are a kind of artificial micro-nano structures that can control and confine the propagation of electromagnetic (EM) waves, and have attracted considerable attention in recent decades.[1–19]

It is well known that in quantum mechanics observable mechanical quantity operators must be Hermitian in order to ensure their eigenvalues are real numbers. However, Bender *et al.*[1] found that for a PT-symmetric mechanical system, when the imaginary part of the potential function is smaller than some critical value, even if the Hamiltonian is non-Hermitian, all of the energy eigenvalues are still real numbers; only when the imaginary part of the potential function is larger than this critical value do its energy eigenvalues start to appear as complex numbers. This critical value is called the spontaneous PT-symmetric breaking point. In 2007, under the condition of paraxial approximation El-Ganainy *et al.*[2] introduced a PT-symmetric optical system by use of materials with even-function real part and odd-function imaginary part refractive indices. Since then, many extraordinary optical properties and phenomena in PT-symmetric systems have been investigated, such as energy transfer oscillation,[3,4] transmission noncommutability,[5,6] unidirectional invisibility,[7,8,20] birefringence,[3,9] defect state,[10] bound states in the continuum (BIC)[11,12] and ultrastrong transmission and reflection.[13–15,21,22]

Optical waveguide networks[23–25] are another kind of artificial micro-nano structure that can control and confine the propagation of EM waves, and are also a kind of photonic band gap (PBG) systems. Compared with photonic crystals, the structure symmetry of optical waveguide networks is much more flexible,[25,26] the phase and amplitude measurements of the EM waves in the latter are also much more convenient,[24] the PBGs generated by the latter can be much wider and deeper than those produced by the former.[26–30] Optical waveguide networks have been widely researched by now; an incomplete list includes strong photonic localization,[31–33] large PBGs,[26–30] comb-like optical transmission spectra,[34,35] nonlinear optical effect,[36–38] and so on.

Combining the PT-symmetric concept with optical waveguide networks, our group designed a PT-symmetric Thue–Morse aperiodic optical waveguide network.[15] We found that the propagation of EM waves in this aperiodic network produces more photonic modes and the concept of spontaneous PT-symmetric breaking point needs to be generalized. The aperiodic network determined by the new defining PT-symmetric breaking point can generate ultrastrong ex-

†Corresponding author. E-mail: xubohu@scau.edu.cn
‡Corresponding author. E-mail: xbyang@scnu.edu.cn

© 2026 Chinese Physical Society and IOP Publishing Ltd. All rights, including for text and data mining, AI training, and similar technologies, are reserved.

traordinary transmission and reflection whose values can, respectively, arrive at 2.96316×10^5 and 1.32761×10^5.[15] However, for aperiodic networks, seeking the spontaneous PT-symmetric breaking points is very complicated. Consequently, for periodic networks, does there exist a more concise and rigorous method to obtain the spontaneous PT-symmetric breaking point for generating ultrastrong extraordinary transmission and reflection? Can periodic networks generate much stronger transmission and reflection than those of aperiodic networks? If so, what is the underlying mechanism responsible for such ultrastrong extraordinary transmission and reflection? Addressing these questions may deepen people's knowledge on PBG materials and PT-symmetric optical systems.

Now, it is known that periodic networks can generate absolute PBGs which are much wider than those created by photonic crystals, and the most typical network is a periodic triangular network,[26] which not only possesses a very simple structure but also generates a very wide PBG with the center gap ratio of 146%.[30] Furthermore, Tang *et al.*[31] found that a defect triangular network can produce ultrastrong photonic localization. In this paper, we replace the vacuum/dielectric waveguide segments in previous triangular networks with the PT-symmetric ones to design a PT-symmetric periodic triangular optical waveguide network (PTSPTOWN) and investigate its extraordinary optical properties. It is found that in this network the EM waves can generate neither ordinary photonic propagation mode nor single gain/loss photonic non-propagation mode, but two kinds of photonic non-propagation modes with co-existing gain and loss in the total range of frequency. Consequently, we reclassify photonic modes and use the distribution diagram of photonic modes to directly seek extremum spontaneous PT-symmetric breaking points/extremum boundary points of photonic modes. Unlike purely numerical calculations commonly adopted in studies of aperiodic networks, our method is directly derived from an analytical formulation of the dispersion function, making the identification of extremum boundary points both concise and physically rigorous. We find that at extremum boundary points of photonic modes, our designed PT-symmetric network can produce ultrastrong extraordinary transmission and reflection, whose values can all arrive at 8.76×10^{11} and are six orders of magnitude larger than those in aperiodic networks.[15] Moreover, we also investigate the mechanism for generating ultrastrong extraordinary transmission in the view of effective refractive index and photonic group velocity. It may provide the theoretical and experimental basis for the design of all-optical devices, such as optical amplifiers, ultra-narrowband optical filters, high-efficiency photonic energy storage, optical logic elements in photon computers, and ultrasensitive optical switches with ultrahigh monochromaticity. On the other hand, the structure of our designed 1D PTSPTOWN is very simple, and the imaginary part of the refractive index of the waveguide material is very small. It may be realized conveniently in experiments.

This paper is organized as follows. Section 2 introduces PTSPTOWN and the main theory and method for analytical deduction and numerical calculation. Section 3 defines the photonic mode by the dispersion relation, obtains the ultrastrong extraordinary optical properties, and discusses the results. Section 4 provides the conclusion of this paper.

2. Model and theory

2.1. PTSPTOWN

The PTSPTOWN studied in this paper is shown in Fig. 1, where the waveguide segments at the entrance and exit are all vacuum ones with the length of d, those in the triangle unit cell are all PT-symmetric ones with the length of d. For simplicity, we set $d = 1$ μm. In unit cells, between each pair of nearest-neighbor nodes there exist two PT-symmetric waveguide segments, which means this is a two-segment-connected network. Each PT-symmetric waveguide segment is made up of SiO_2 and consists of three equal-length sub-waveguides, whose refractive indices are, respectively, $n_1 = n_{SiO_2} - \imath n_I$, $n_2 = n_{SiO_2}$ and $n_3 = n_{SiO_2} + \imath n_I$. Here the complex conjugate refractive indices along the length can be achieved by doping the gain and loss quantum dots.[13,39]

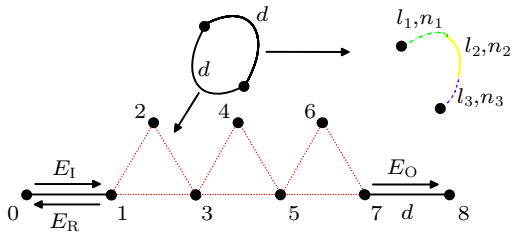

Fig. 1. Schematic diagram of the PTSPTOWN with three unit cells, one entrance, and one exit, where each dotted line denotes two PT-symmetric waveguide segments with the length of d. Each waveguide segment consists of three equal-length sub-waveguides whose refractive indices are n_1, n_2, and n_3, respectively. Each solid line represents one vacuum waveguide segment with the length of d. E_I, E_R, and E_O are the input, reflective, and output EM waves, respectively.

It is reported that in the range of 43–1427 THz (i.e., 0.21–7.00 μm), the dispersion equation of SiO_2 satisfies[40]

$$n_{SiO_2}^2 - 1 = \frac{0.6961663\lambda^2}{\lambda^2 - 0.0684043^2} + \frac{0.4079426\lambda^2}{\lambda^2 - 0.1162414^2} + \frac{0.8974794\lambda^2}{\lambda^2 - 9.896161^2}, \tag{1}$$

and the dispersion curve is plotted in Fig. 2.

From Fig. 2 one can see that in the range of 200–500 THz (i.e., 0.6–1.5 μm), the dispersion effect is weak. In order to reduce the workload and the influence of the dispersion effect on the results, only the EM waves with the frequency (wavelength) in the range of 300–500 THz (0.6–1.0 μm) are studied, which corresponds to the dispersion curve of the thick red solid line in Fig. 2.

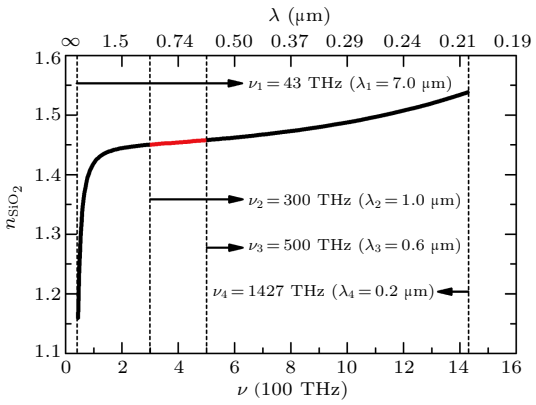

Fig. 2. Dispersion curve of SiO_2 defined by Eq. (1), where the red thick solid line expresses the range investigated in this paper, the black thin dashed lines are all scaling lines and the values are, respectively, $\nu_1 = 43$ THz ($\lambda_1 = 7.0$ μm), $\nu_2 = 300$ THz ($\lambda_2 = 1.0$ μm), $\nu_3 = 500$ THz ($\lambda_3 = 0.6$ μm), and $\nu_4 = 1427$ THz ($\lambda_4 = 0.2$ μm).

2.2. Three-material network equation

From Fig. 1 one can see that in a PT-symmetric network, each waveguide segment in unit cells is composed of three kinds of materials. Consequently, a three-material network equation must be used to investigate the PTSPTOWN. In this section, we derive the three-material network equation specifically for our designed two-segment-connected PTSPTOWN with equal waveguide length.

It is known that the EM wave function with frequency ν in the three-material segments satisfies the following wave equation:

$$\frac{\mathrm{d}^2}{\mathrm{d}x^2}\psi_{n_m}(x) + k_m^2\psi_{n_m}(x) = 0, \tag{2}$$

where the EM wave vector $k_m = 2\pi\nu n_m/c$ ($m = 1, 2, 3$), n_m is the refractive index of the mth kind of material, c is the EM wave speed in vacuum.

For a 1D waveguide segment, only the monomode propagation of EM waves needs to be considered. The wave function between nodes i and j can be regarded as the following linear combination of two oppositely traveling plane waves:

$$\psi_{ij}(x) = \begin{cases} \psi_{n_1}(x) = a_1\mathrm{e}^{\imath k_1 x} + b_1\mathrm{e}^{-\imath k_1 x}\,(0 \le x \le l_1 l_{ij}), \\ \psi_{n_2}(x) = a_2\mathrm{e}^{\imath k_2 x} + b_2\mathrm{e}^{-\imath k_2 x}\,(l_1 l_{ij} \le x \le l_{12} l_{ij}), \\ \psi_{n_3}(x) = a_3\mathrm{e}^{\imath k_3 x} + b_3\mathrm{e}^{-\imath k_3 x}\,(l_{12} l_{ij} \le x \le l_{ij}), \end{cases} \tag{3}$$

where $l_{12} = l_1 + l_2$, l_{ij} is the total length of the waveguide segment with three kinds of materials. Applying the continuity of the wave function and its derivative, the energy flux conservation at any node yields

$$\sum_j \frac{\sigma_{ij}}{\mu\omega}\psi_{ij}(x)\frac{\mathrm{d}\psi_{ij}(x)}{\mathrm{d}x}\bigg|_{x=0} = 0, \tag{4}$$

where the summation is over all segments linked directly to node i. Generally, the cross-sectional area σ_{ij} for each segment is the same. By means of Eqs. (3) and (4), one can deduce the following network equation of three-material multi-connected optical waveguide networks

$$\begin{aligned} &-\psi_i\sum_j \frac{A_1B_1\cos D_1 l_{ij} - A_1B_2\cos D_2 l_{ij} - A_2B_1\cos D_3 l_{ij} + A_2B_2\cos D_4 l_{ij}}{A_1B_1\sin D_1 l_{ij} - A_1B_2\sin D_2 l_{ij} - A_2B_1\sin D_3 l_{ij} + A_2B_2\sin D_4 l_{ij}} \\ &+\sum_j \psi_j \frac{4k_2k_3}{A_1B_1\sin D_1 l_{ij} - A_1B_2\sin D_2 l_{ij} - A_2B_1\sin D_3 l_{ij} + A_2B_2\sin D_4 l_{ij}} = 0, \end{aligned} \tag{5}$$

where

$$\begin{cases} A_1 = k_1 + k_2, \\ A_2 = k_1 - k_2, \\ B_1 = k_2 + k_3, \\ B_2 = k_2 - k_3, \\ D_1 = k_1 l_1 + k_2 l_2 + k_3 l_3, \\ D_2 = k_1 l_1 + k_2 l_2 - k_3 l_3, \\ D_3 = k_1 l_1 - k_2 l_2 - k_3 l_3, \\ D_4 = k_1 l_1 - k_2 l_2 + k_3 l_3. \end{cases} \tag{6}$$

Since PT-symmetric networks represent a class of three-material waveguide networks, we employ Eqs. (5) and (6) to analyze their extraordinary optical properties.

2.3. Generalized Floquet–Bloch theorem and generalized eigenfunction method

It is well-established that the Floquet–Bloch theorem applies to systems with spatial translation periodicity. However, in our designed optical waveguide network, all waveguide segments can be arbitrarily bent or folded, resulting in topological translation periodicity without spatial periodicity. For such structures, we previously proposed a dimensionless generalized Floquet–Bloch theorem, which can be expressed as follows:[25]

$$\psi_{\boldsymbol{K}}(\boldsymbol{N} + \boldsymbol{P}) = \psi_{\boldsymbol{K}}(\boldsymbol{N})\,\mathrm{e}^{\imath\boldsymbol{K}\cdot\boldsymbol{P}}, \tag{7}$$

where $\boldsymbol{K}$ is the structure Bloch wavevector, $\boldsymbol{N}$ is the node scaling vector, and $\boldsymbol{P}$ is the structure translation vector. The three vectors are all dimensionless. In this paper, we use the dimensionless generalized Floquet–Bloch theorem to deduce the dispersion relation, define photonic modes, and determine the distribution of photonic modes.

Additionally, the generalized eigenfunction method[29] is employed to calculate transmissivity and reflectivity, where transmission and reflection coefficients act as generalized wave functions.

3. Extraordinary optical properties

3.1. Extraordinary photonic modes

According to the generalized Floquet–Bloch theorem, when EM waves propagate from the Nth unit cell to the $(N+P)$th unit cell, the only difference between the wave function of the former and that of the latter is the phase factor of $e^{\iota \boldsymbol{K}\cdot\boldsymbol{P}}$. For our designed PTSPTOWN, one can deduce the following dispersion relation by putting Eq. (5) into Eq. (7):

$$\cos K = f(\nu) = \frac{4Y^2 - Z^2}{2YZ + Z^2}, \tag{8}$$

where

$$\begin{cases} Y = \sum\limits_j \dfrac{A_1B_1\cos D_1 l_{ij} - A_1B_2\cos D_2 l_{ij} - A_2B_1\cos D_3 l_{ij} + A_2B_2\cos D_4 l_{ij}}{A_1B_1\sin D_1 l_{ij} - A_1B_2\sin D_2 l_{ij} - A_2B_1\sin D_3 l_{ij} + A_2B_2\sin D_4 l_{ij}}, \\ Z = \sum\limits_j \dfrac{4k_2k_3}{A_1B_1\sin D_1 l_{ij} - A_1B_2\sin D_2 l_{ij} - A_2B_1\sin D_3 l_{ij} + A_2B_2\sin D_4 l_{ij}}. \end{cases} \tag{9}$$

From Eq. (8) one can see that for a three-material multiconnected network composed of vacuum and/or dielectric waveguides, the dispersion function $f(\nu)$ must be real. In the case of real $f(\nu)$ and $|f(\nu)| \le 1$, the $\boldsymbol{K}$ in Eq. (8) possesses real solutions, and then the amplitude of the wavefunctions does not change with the propagation; we refer to this photonic mode of EM waves as ordinary propagation mode. It forms passbands and causes large transmission that is sustained even with an increasing number of unit cells and, generally, $0.01 \le T_{\text{passband}} \le 1.0$.[25,26,41] In the case of real $f(\nu)$ and $|f(\nu)| > 1$, the $\boldsymbol{K}$ in Eq. (8) possesses a pair of complex conjugate solutions, and then the amplitude of the wavefunctions changes with the propagation; we refer to this photonic mode of EM waves as non-propagation mode. In a vacuum/dielectric network, there exists only attenuation mechanism but no gain mechanism; thus EM waves propagate with attenuation propagation mode, which forms a stopband and causes a tiny transmission decreasing with the increase of the number of unit cells and, generally, $T_{\text{stopband}} < 0.01$.[25,26,41] One can see that in a vacuum/dielectric network, $|f(\nu)| = 1$ can be used for the critical value to distinguish photonic modes. In our designed PTSPTOWN, the refractive indices of two kinds of materials form a complex-conjugate pair; one can deduce that the dispersion function will be also complex in the total range of frequency. In the case of complex $f(\nu)$, the $\boldsymbol{K}$ in Eq. (8) possesses no real solution but a pair of complex conjugate solutions. From the aspect of mathematics, EM waves in this PT-symmetric network will propagate as attenuation and gain propagation modes simultaneously. On the other hand, in PT-symmetric optical waveguides, both attenuation and gain mechanisms exist. Consequently, from the aspect of physics, EM waves will propagate as attenuation and gain propagation modes simultaneously. It means that in this PT-symmetric network the $\boldsymbol{K}$ possesses no real solution but a pair of complex conjugate ones, and then no matter whether the transmissivity decreases with the increment of the number of unit cells and whichever range the EM wave frequency is, the traditional passbands and/or stopbands will not exist now.

On the other hand, it is reported that the spontaneous PT-symmetric breaking point is located at the boundary between the ordinary propagation mode and non-propagation mode.[15] However, in our designed PTSPTOWN there is no propagation mode, so we still use $|f(\nu)| = 1$ as a critical point to distinguish photonic modes. From Eq. (8) one knows that when $|f(\nu)| > 1$, the imaginary part of $\boldsymbol{K}$ will be big enough to generate strong extraordinary transmission whose value is larger than 1.0, and we define this kind of photonic modes as strong propagation modes. When $|f(\nu)| \le 1$, the imaginary part of $\boldsymbol{K}$ is small and cannot produce strong extraordinary transmission whose value is larger than 1.0, and we define this kind of photonic modes as weak propagation modes. Obviously, both strong and weak propagation modes belong to a category of non-propagation modes, which are distinct not only from ordinary propagation modes but also from the non-propagation modes originating from vacuum or dielectric networks. In this paper, we define the value of the imaginary part of the PT-symmetric materials, n_{I}, as the boundary point of photonic modes between strong propagation modes and weak propagation modes, and use this definition to investigate the distribution of photonic modes in Subsection 3.2.

3.2. Extremum boundary point of photonic mode

Based on the definitions of strong and weak propagation modes in Subsection 3.1 and the boundary point of photonic mode in PTSPTOWN, we use Eq. (8) to plot the distribution diagram of photonic modes for the EM waves in the range of 300–500 THz.

From Fig. 3, one can see that there exists one extremum valley for the boundary point of photonic modes of PTSPTOWN, and we call it the extremum boundary point of the photonic mode, located at $n_{\text{I}} = 8.809 \times 10^{-9}$ and $\nu = 412.172102$ THz. At this point, $|f(\nu)| = 1$ and the dispersion function $f(\nu)$ is continuous without a derivative. It causes ultrastrong extraordinary optical transmission and reflection.

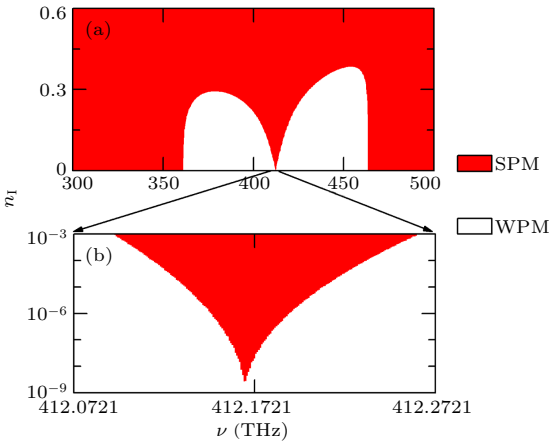

Fig. 3. Distribution diagram of photonic modes, where red and white zones express strong and weak propagation modes, respectively. (a) The frequency range corresponds to the thick red solid line in Fig. 2. (b) The enlarged drawing of the zone of the frequency range from 412.0721 THz to 412.2721 THz.

3.3. Ultrastrong extraordinary transmission and reflection

In order to investigate the transmission and reflection of EM waves propagating in the PTSPTOWN, we numerically calculate the transmissivity and reflectivity in the range of 300–500 THz. It is found that the transmissivity and reflectivity in regimes corresponding to the pure weak or strong propagation modes are generally smaller than those at the boundary point of photonic modes; the former is usually smaller than 1.0 while the latter is always bigger than 1.0. The transmissivity and reflectivity at the boundary point of photonic modes are much smaller than those at the extremum boundary point of photonic modes; the former is generally smaller than 10^5 while the latter's maximum can arrive at 10^{11}.

From the aforementioned analyses one knows that ultrastrong extraordinary transmission and reflection can be generated at the extremum boundary point of photonic modes. Therefore, we further investigate the transmissivity and reflectivity for a PTSPTOWN with one unit cell at the point where this extremum occurs, and the results are presented in Fig. 4.

From Fig. 4(a) one can see that there are two sharp transmissivity valleys, and the values for both left- and right-incident EM waves are all the same and arrive at 3.77×10^{-12}, which shows an ultrastrong PBG-like attenuation characteristic. On the other hand, from Fig. 4(a) one can also see that there are two transmissivity peaks for left- and right-incident EM waves and the values are, respectively, 8.76×10^{11} and 7.46×10^{11}, which are six orders of magnitude larger than that created by aperiodic networks. The case of reflection is similar to that of transmission. From Fig. 4(b) one can see that there exists no reflectivity valley, but only two reflectivity peaks exist and the values for left- and right-incident EM waves arrive at 8.76×10^{11} and 7.46×10^{11}, respectively. From Fig. 4 one can see that for both transmissivity and reflectivity, the left- and right-incident curves do not overlap each other, which shows typical noncommutability of EM wave propagation in the PTSPTOWN. In such a system, both the transmitted and reflected waves can exhibit an ultrastrong resonant coupling effect, giving rise to sharp resonance peaks.

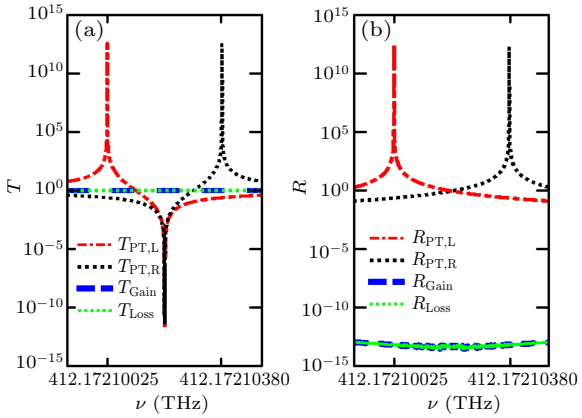

Fig. 4. Transmission and reflection spectra at the extremum boundary point of photonic mode of periodic triangular network with one unit cell, where red dashed and dotted lines and black thick dotted lines express left- and right-incident results of PT-symmetric network, respectively, blue thick dashed lines denote the results of pure gain-material network with the refractive index $n_{\mathrm{Gain}} = n_{\mathrm{SiO_2}} - 8.809\times10^{-9}\imath$, green thin dotted lines indicate the results of pure loss-material network with the refractive index $n_{\mathrm{Loss}} = n_{\mathrm{SiO_2}} + 8.809\times10^{-9}\imath$. (a) Transmission spectra. (b) Reflection spectra.

In our opinion, there are two main reasons for the PTSPTOWN generating the ultrastrong extraordinary transmission and reflection. Firstly, from the analyses on the extraordinary photonic modes in Subsection 3.1 one can see that the structure Bloch wavevector possesses no real solution but only a pair of complex conjugate solutions. Consequently, there exists no ordinary propagation mode but two kinds of non-propagation modes, strong and weak propagation modes. These two kinds of non-propagation modes are different from the ordinary propagation mode and attenuation propagation mode produced by vacuum/dielectric networks. Thus the transmission and reflection spectra of the PTSPTOWN are completely different from those of vacuum/dielectric networks. Secondly, for photons there exists no single gain and/or loss mode, but only resonant coupling effect on photonic modes. Furthermore, compared with reported PT-symmetric optical systems, when EM waves propagate in the PTSPTOWN, it will produce multi-quantum coherent superposition, which will further strengthen the aforementioned resonant coupling effect, then the ultrastrong extraordinary transmission and reflection are generated.

In order to investigate the resonant coupling effect of gain and loss in PT-symmetric networks, we compare the transmissivity and reflectivity in PT-symmetric networks with those in the networks composed of single gain and loss materials. Thus we calculate the transmissivity and reflectivity of the periodic triangle networks composed of single gain or loss materials, whose refractive indices are $n_{\mathrm{Gain}} = n_{\mathrm{SiO_2}} - 8.809\times10^{-9}\imath$ or $n_{\mathrm{Loss}} = n_{\mathrm{SiO_2}} + 8.809\times10^{-9}\imath$, respectively. From Fig. 4(a)

one can see that the transmissivity of the network composed of single gain material (the blue thick dashed line) is approximately 1.0001, and that of the network composed of single loss material (the green thin dotted line) is approximately 0.9998. The network composed of single gain materials generates an extraordinary transmission which is greater than 1.0, but it is far less than the ultrastrong extraordinary transmission generated by the PT-symmetric network with the same imaginary part which arrives at the order of 10^{11}. The network composed of single loss materials generates a transmission which is smaller than 1.0, but it is much bigger than the transmission generated by the PT-symmetric network with the same imaginary part which arrives at the order of 10^{-12}. From Fig. 4(b) one can see that the reflectivity of the network composed of single gain (the blue thick dashed line) or loss (the green thin dotted line) materials arrives at the order of 10^{-14}; it is far less than the reflection produced by the PT-symmetric network with the same imaginary part which arrives at the order of 10^{11}. It means that the gain and loss effects for transmission and reflection in the single gain or loss materials are far smaller than those in the PT-symmetric network; furthermore, we set the imaginary part of the gain or loss material to be very small (only 10^{-9} order), so the pure gain or loss effect is very weak.

For this reason, in PT-symmetric networks, the gain or loss effects of both single gain and loss materials are all negligible and play a very minor role; they will neither cancel nor weaken each other, but both couple and strengthen each other under the multiple coupling effects of gain and loss effects. The gain and loss materials in each PT-symmetric optical waveguide together form a coupled resonator system. This system creates a strong resonant coupling effect for the photons propagating through the network, resulting in sharp resonance peaks and valleys in the spectrum. Their resonant frequencies are determined by the network structure. Because of the noncommutability of EM wave propagation, the resonance peaks for left- and right-incident do not coincide with each other. In addition, the quantum coherence superposition effect inherent to PT-symmetric networks can strengthen the mechanism of resonant coupling, leading to a more pronounced effect. Therefore, it can generate ultrastrong extraordinary transmission and reflection in PTSPTOWN.

Our further research shows that the ultrastrong extraordinary transmission and reflection at the extremum boundary points of photonic modes are also closely related to the number of unit cells. As examples, we calculate the transmission/reflection for left-incident EM waves at the extremum boundary points of photonic modes in the PTSPTOWN with 1 to 8 unit cells and list the results in Table 1.

Table 1 illustrates the evolution of transmission and reflection at the extremum boundary points of the photonic modes as the number of unit cells increases. In the left column, both the transmissivity and frequency of the peaks decrease, meaning the peaks diminish and shift toward lower frequencies. The middle column shows that while the transmissivity of the valleys decreases, their frequency remains constant at 412.17210205 THz. Similarly, the right column indicates that the reflectivity and frequency of the peaks also decrease, resulting in the peaks that are likewise shifted to lower frequencies.

Table 1. Transmissions/reflections of PTSPTOWN at the extremum boundary points of photonic modes for different unit cell numbers, where N expresses the unit cell number, T_{peak} and $\nu_{T_{\text{peak}}}$ express the transmissivity and frequency of the left-incident transmission peak, T_{valley} and $\nu_{T_{\text{valley}}}$ express the transmissivity and frequency of the left-incident transmission valley, and R_{peak} and $\nu_{R_{\text{peak}}}$ express the reflectivity and frequency of the left-incident reflection peak.

N	$T_{\text{peak}}(\nu_{T_{\text{peak}}})$	$T_{\text{valley}}(\nu_{T_{\text{valley}}})$	$R_{\text{peak}}(\nu_{R_{\text{peak}}})$
1	8.76×10^{11}(412.17210025)	3.77×10^{-12}(412.17210205)	8.76×10^{11}(412.17210025)
2	4.79×10^{11}(412.17209848)	6.19×10^{-12}(412.17210205)	4.79×10^{11}(412.17209848)
3	4.82×10^{11}(412.17209670)	2.16×10^{-13}(412.17210205)	4.82×10^{11}(412.17209670)
4	1.37×10^{11}(412.17209493)	1.55×10^{-13}(412.17210205)	1.37×10^{11}(412.17209493)
5	6.04×10^{10}(412.17209316)	7.78×10^{-14}(412.17210205)	6.04×10^{10}(412.17209316)
6	2.96×10^{10}(412.17209141)	6.89×10^{-14}(412.17210205)	2.96×10^{10}(412.17209141)
7	1.62×10^{10}(412.17208962)	3.87×10^{-15}(412.17210205)	1.62×10^{10}(412.17208962)
8	9.46×10^{9}(412.17208785)	5.06×10^{-15}(412.17210205)	9.46×10^{9}(412.17208785)

3.4. Effective refractive index

In order to investigate the mechanism of the ultrastrong extraordinary transmission and ultraweak transmission produced by the PTSPTOWN, we take example by the mechanism of the extraordinary transmission created by photonic crystals by introducing effective refractive index.[42,43] It is well known that the transmission coefficient t and transmissivity T of an optical waveguide network satisfy the following relationship:

$$t = \sqrt{T}\,\mathrm{e}^{\mathrm{i}\Phi_t} = \mathrm{e}^{\mathrm{i}\frac{\omega n_{\text{eff}} L}{c}}, \tag{10}$$

where the total cumulative phase $\Phi_t = \arctan(t_{\text{I}}/t_{\text{R}}) \pm m\pi$, m is integer. t_{I} and t_{R} are the real and imaginary parts of the transmission coefficient, respectively, L is the effective length of the network, n_{eff} is the effective refractive index and can be

expressed as follows:

$$n_{\text{eff}} = \eta + \iota\gamma, \tag{11}$$

where

$$\begin{cases} \eta = \dfrac{c\Phi_t}{\omega L}, \\ \gamma = -\dfrac{c\ln T}{2\omega L}. \end{cases} \tag{12}$$

Obviously, η represents the effective phase of EM waves; γ denotes the gain or loss effect for the amplitude of EM waves.

For photonic crystals, the group velocity of EM waves is defined as $v_{\text{g-PC}} = \mathrm{d}\omega/\mathrm{d}k$.[42,43] In our designed PT-symmetric network, we change the refractive index, n, into the real part of the effective refractive index, η, and redefine the group velocity as $v_{\text{g-PT}} = \mathrm{d}(2\pi\nu)/\mathrm{d}(2\pi\nu\eta/c) = c/(\eta + \nu\mathrm{d}\eta/\mathrm{d}\nu)$. Taking the example of the definition of phase velocity, $v_{\text{p}} = c/n$, we simplify the expression of the group velocity of PT-symmetric networks as

$$v_{\text{g-PT}} = \frac{c}{n_{\text{g}}}, \tag{13}$$

where we call n_{g} the group refractive index and define it as $n_{\text{g}} = |\eta + \nu\mathrm{d}\eta/\mathrm{d}\nu|$.

In order to investigate the mechanism of the ultrastrong extraordinary transmission produced by PT-symmetric networks, we numerically calculated the real and imaginary parts of the effective refractive index and group refractive index of the left-incident EM wave at the extremum boundary points of the photonic modes of PTSPTOWN with one unit cell, respectively. The results are shown in Fig. 5.

From Fig. 5(a) one can see that at the frequency of $\nu_1 = 412.17210025$ THz, there exists an ultrastrong transmission peak whose value arrives at 8.76×10^{11}; at the frequency of $\nu_2 = 412.17210380$ THz, there exists an ultradeep transmission valley whose value arrives at 3.77×10^{-12}. From Fig. 5(b) one can see that at the frequency ν_1, there exists a γ valley whose value is -0.620; at the frequency ν_2, there exists a γ peak whose value is 0.613. Comparing Figs. 5(a) and 5(b), one can see that the frequencies of the ultrastrong transmission peak and ultradeep transmission valley precisely correspond to those of the valley and peak of γ, respectively. It means that the ultrastrong and ultraweak transmissions are, respectively, caused by the total gain and loss effects of PT-symmetric materials and network structures, and it also demonstrates that the definition of effective refractive index is suitable for PT-symmetric networks and may be useful for explaining the gain and/or loss transmission of PT-symmetric optical waveguide networks.

From Figs. 5(c) and 5(d) one can see that at the frequency ν_1, there exists an ultrastrong peak of group refractive index, whose value reaches $n_{\text{g}} = 1.385\times10^8 \gg 1.0$. Then based on Eq. (13) one can deduce that at ν_1, the group velocity of the EM waves propagating in our designed PTSPTOWN is $v_{\text{g-PT}} \approx 7.220\times10^{-9}c \ll c$. Obviously, it is a very slow photonic group velocity, and this distinct slow light effect will cause remarkable photonic accumulations, and consequently, ultrastrong extraordinary optical transmission is produced.

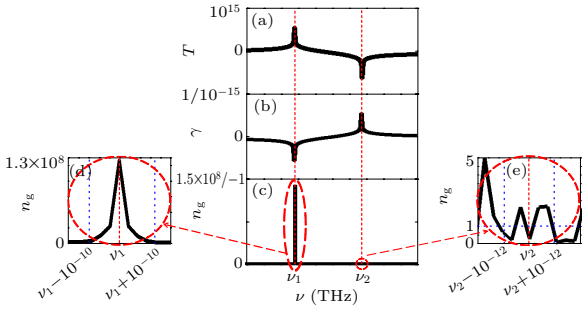

Fig. 5. Three kinds of spectra of left-incident EM waves at the extremum boundary points of photonic modes in PTSPTOWN with one unit cell, where T is the transmissivity, γ is the imaginary part of n_{eff}, n_{g} is the group refractive index, $\nu_1 = 412.17210025$ THz, $\nu_2 = 412.17210380$ THz. (a) Transmission spectra. (b) γ spectra. (c) Group refractive index spectra. (d) and (e) Enlarged diagrams of the left- and right-sides of (c), respectively.

On the other hand, from Fig. 5(c) one can also see that at the frequency ν_2, there exists no obvious fluctuation, but from Fig. 5(e), the enlarged diagram of Fig. 5(c) near the frequency ν_2, one can see a small fluctuation at frequency ν_2 whose peak value is $n_{\text{g}} = 0.2537 < 1.0$. Then based on Eq. (13) one can deduce that at the frequency ν_2, the group velocity of the EM waves propagating in our designed PTSPTOWN is $v_{\text{g-PT}} \approx 3.942c > c$. Obviously, it is a fast photonic group velocity, and this fast light effect will cause a remarkable photonic loss effect.

In brief, the step of the imaginary part of the effective refractive index exactly corresponds to that of transmissivity. It means that the definition of the effective refractive index is suitable for PT-symmetric optical waveguide networks, and just as in general media/photonic crystals, the imaginary part of the effective refractive index of PT-symmetric optical waveguide networks still corresponds to the total gain and loss effect of the network. However, the step of the real part of the effective refractive index does not exactly correspond to that of transmissivity. It means that the real part of the effective refractive index of PT-symmetric optical waveguide networks does not correspond to the total photonic phase of the network. We think the reason is as follows. In a PT-symmetric network, the waveguide connections among nodes are very complex, and then when EM waves propagate in the system, the quantum coherent superposition effect may lead to the effective phase of the total network being complex and random; slow photonic group velocity and the corresponding slow light effect are certain, but fast photonic group velocity and the corresponding fast and/or super-fast light effect are disordered and uncertain.

Furthermore, a relationship exists between the transmission and reflection in PT-symmetric systems, as shown in Ref. [19]: $\sqrt{R_{\rm L}R_{\rm R}} = |1-T|$. When $T \gg 1$, the product of the left and right reflectivities equals the square of the transmissivity, i.e., $R_{\rm L}R_{\rm R} = T^2$. Although the non-reciprocal nature of PT-symmetric systems results in $R_{\rm L} \neq R_{\rm R}$, an ultrastrong transmissivity peak (with $T \gg 1$) is always accompanied by ultrastrong reflection at the same frequency. Therefore, the correspondence between the imaginary part of the effective refractive index and ultrastrong transmission is completely analogous to its correspondence with ultrastrong reflection.

4. Conclusions

In this paper, we design an interesting PTSPTOWN, investigate the ultrastrong extraordinary transmission and reflection, and try to explain the mechanism of the extraordinary optical characteristics by means of effective refractive index and group velocity.

First, we investigate the photonic modes in PTSPTOWN. It is found that periodic PT-symmetric networks are better than aperiodic PT-symmetric networks. In a variety of coupling effects, the photonic modes in PT-symmetric networks consist of two kinds of non-propagation modes with coexisting gain and loss in the total range of frequency. As a result, we reclassify the photonic modes to obtain extremum boundary points of photonic modes which generate ultrastrong extraordinary transmission and reflection. This method is more concise and rigorous than that in aperiodic PT-symmetric networks.

Second, we numerically calculate the ultrastrong extraordinary transmission and reflection generated by PTSPTOWN. It is found that, at the extremum boundary points of photonic modes, the EM wave can generate ultrastrong extraordinary transmission and reflection, which are more than 6 orders of magnitude greater than that of aperiodic PT-symmetric networks. From the perspective of physical mechanism, EM waves propagating in the PT-symmetric system formed by materials with complex-conjugate imaginary parts of the refractive index produce intense resonance, which further induces the slow light effect. Meanwhile, the resonant enhancement together with the gain leads to the accumulation of photonic energy. These peculiar phenomena and properties are conducive to the design and development of extremely narrow filters, optical switches, high-efficient photon storage, and other all-optical devices.

Finally, we introduce the effective refractive index of PT-symmetric networks and explore the relationship between the real and imaginary parts of the effective refractive index and the ultrastrong extraordinary transmission. It is found that the gain and loss effects defined by the imaginary part of the effective refractive index directly correlate with the ultrastrong extraordinary transmission. In contrast, there is no definite corresponding relationship between the group velocity defined by the real part of the effective refractive index and the ultrastrong extraordinary transmission. We believe that this is due to the complex quantum coherence effect of the PT-symmetric network; the phase generated by EM waves in a PT-symmetric network is more complex than that of a PT-symmetric optical system with a single optical path. Therefore, the effective phase of the whole network is very disorganized. These findings deepen people's understanding of photon propagation in artificial microstructures and provide insights into the relationship between extraordinary optical properties, effective refractive index, and group velocity.

Acknowledgements

Project supported by the Natural Science Foundation of Guangdong Province (Grant No. 2018A0303130232) and the National Natural Science Foundation of China (Grant No. 11674107).

References

[1] Bender C M, Boettcher S 1998 *Phys. Rev. Lett.* **80** 5243
[2] El-Ganainy R, Makris K G, Christodoulides D N and Musslimani Z H 2007 *Opt. Lett.* **32** 2632
[3] Makris K G, El-Ganainy R, Christodoulides D N and Musslimani Z H 2008 *Phys. Rev. Lett.* **100** 103904
[4] Longhi S 2009 *Phys. Rev. Lett.* **103** 123601
[5] Kala M, Singh P and Mishra A K 2025 *Opt. Commun.* **579** 131521
[6] Jaseera C P, Muhsina K A and Thasneem A R 2025 *Chaos* **35** 023154
[7] Lin Z, Ramezani H, Eichelkraut T, Kottos T, Cao H and Christodoulides D N 2011 *Phys. Rev. Lett.* **106** 213901
[8] Jin L, Zhang X Z, Zhang G and Song Z 2016 *Sci. Rep.* **6** 20976
[9] Tao L, Wang F, Wu Z and Xia G 2023 *IEEE Access* **11** 23127
[10] Regensburger A, Miri M A, Bersch C, Näger J, Onishchukov G, Christodoulides D N and Peschel U 2013 *Phys. Rev. Lett.* **110** 223902
[11] Song Q, Yi Z, Xiang H and Han D 2025 *Phys. Rev. A* **112** 063517
[12] Zhou Q, Long Q, Hu J, Shao W and Xu Y 2025 *Chin. Phys. Lett.* **42** 120402
[13] Ding S and Wang G P 2015 *J. Appl. Phys.* **117** 023104
[14] Fan Y, Yang X, Lian H, Chen R, Zhu P, Deng D, Liu H and Wei Z 2024 *Chin. Phys. B* **33** 034201
[15] Wu J and Yang X 2017 *Opt. Express* **25** 27724
[16] Thasneem A R, Subha P A and Muhsina K A 2024 *J. Mod. Opt.* **71** 63
[17] Lin Z, Song W, Wang L, Xin H, Sun J, Wu S, Huang C, Zhu S, Jiang J and Li T 2024 *Phys. Rev. Lett.* **133** 073803
[18] Bentzien J, Pinske J, Maczewsky L J, Weimann S, Heinrich M, Scheel S and Szameit A 2025 *Nat. Commun.* **16** 8225
[19] Lin Y, Yang X, Zhang R, Huang C, Deng D, Liu H and Wei Z 2023 *Opt. Express* **31** 30932
[20] Kuang S, Yang X, Lin Y, Wang Y, Dong J, Deng D, Liu H and Wei Z 2026 *Opt. Laser Technol.* **196** 114716
[21] Ma J, Yang X, Huang M, Liang X, Deng D, Liu H and Wei Z 2023 *Commun. Nonlinear Sci.* **118** 106990
[22] Lin Y, Yang X, Zhang R, Huang C, Deng D, Liu H and Wei Z 2024 *Results Phys.* **58** 107529
[23] Vasseur J O, Deymier P A, Dobrzynski L, Djafari-Rouhani B and Akjouj A 1997 *Phys. Rev. B* **55** 10434
[24] Zhang Z Q, Wong C C, Fung K K, Ho Y L, Chan W L, Kan S C, Chan T L and Cheung N 1998 *Phys. Rev. Lett.* **81** 5540
[25] Wang Z and Yang X 2007 *Phys. Rev. B* **76** 235104
[26] Cheung S, Chan T, Zhang Z and Chan C T 2004 *Phys. Rev. B* **70** 125104
[27] Dobrzynski L, Akjouj A, Djafari-Rouhani B, Vasseur J O and Zemmouri J 1998 *Phys. Rev. B* **57** R9388

[28] Mir A, Akjouj A, Vasseur J O, Djafari-Rouhani B, Fettouhi N, Boudouti E H E, Dobrzynski L and Zemmouri J 2003 *J. Phys.: Condens. Matter* **15** 1593
[29] Lu J, Yang X, Zhang G and Cai L 2011 *Phys. Lett. A* **375** 3904
[30] Xiao Q, Yang X, Lu J and Liu C 2012 *Opt. Commun.* **285** 3775
[31] Tang Z, Yang X, Lu J and Liu C T 2014 *Opt. Commun.* **331** 53
[32] Wang N, Yang X, Xu X, Huang Y, Cao P, Deng D, Liu C T and Hu X 2016 *IEEE Photonics J.* **8** 4502513
[33] Hu X, Yang X and Deng D 2017 *IEEE Photonics J.* **9** 4700414
[34] Yang X, Song H and Liu T C 2013 *Phys. Lett. A* **377** 3048
[35] Wang Y, Yang X, Lu J, Zhang G and Liu C T 2014 *Phys. Lett. A* **378** 1200
[36] Zhang M, Yang X, Wang Q, Yao X, Deng D, Liu H and Wei Z 2020 *Opt. Commun.* **474** 126091
[37] Wu J and Yang X 2019 *Ann. Phys-Berlin* **531** 1800258
[38] Hu X, Tang X and Yang X 2024 *Chin. J. Phys.* **87** 804
[39] Feng L, Xu Y, Fegadolli W S, Lu M, Oliveira J E B, Almeida V R, Chen Y and Scherer A 2013 *Nat. Mater.* **12** 108
[40] Malitson I H 1965 *J. Opt. Soc. Am.* **55** 1205
[41] Xu X, Yang X, Wang S, Liu T C and Deng D 2015 *Opt. Express* **23** 27576
[42] Zhu S, Liu N, Zheng H and Chen H 2000 *Opt. Commun.* **174** 139
[43] Liu N, Zhu S, Chen H and Wu X 2002 *Phys. Rev. E* **65** 046607